

7th Asian-Pacific Conference on Aerospace Technology and Science, 7th APCATS 2013

## Vibration analysis of elastically restrained laminated composite sound radiation plates via a finite element approach

C. H. Jiang, T. Y. Kam\*

*Mechanical Engineering Department, National Chiao Tung University, Hsin Chu 300, Taiwan, Republic of China*

---

### Abstract

The vibration characteristics (natural frequencies and vibration shapes) of elastically restrained laminated composite plates used for sound radiation are studied via both theoretical and experimental approaches. The laminated composite sound radiation plates restrained by peripheral and/or interior elastic supports are excited using an electro-magnetic exciter for generating sounds. In the theoretical study, a finite element formulation is presented to model the free and forced vibrations of the elastically restrained laminated composite plate. The present finite element method is then used to study the effects of support conditions, plate aspect ratio, and size ratio of plate length to voice coil radius on the vibration characteristics of the elastically restrained laminated composite sound radiation plates. In the experimental study, several centrally restrained laminated composite plates were subjected to sweep sine excitation to determine the frequency response spectra from which the natural frequencies of the plates were identified. The elastically restrained laminated composite plates with salt powder distributed on their top surfaces were excited to generate the vibration shapes of the plates at several selected frequencies. The experimental results are then used to verify the feasibility and accuracy of the proposed finite element model. The close agreement between the experimental and theoretical results has validated the suitability of the proposed finite element model for vibration analysis of sound radiation plates. The theoretical and experimental results presented in this paper can also serve as benchmarks for verifying the correctness of any analytical model established for vibration analysis of laminated composite sound radiation plates.

© 2013 The Authors. Published by Elsevier Ltd.  
Selection and peer-review under responsibility of the National Chiao Tung University

*Keywords:* Composite materials, laminated plate, natural frequency, vibration, modal analysis, finite element method, elastic support.

---

---

\* Corresponding author. Tel: +886-3-5712121; fax: +886-3-6125057.  
E-mail address: [tykam@mail.nctu.edu.tw](mailto:tykam@mail.nctu.edu.tw)

## 1. Introduction

Laminated composite plates have been widely used in the industries such as aircraft, aerospace, automotive, and audio industries to make high performance structural parts or products. In general, the laminated composite plates used to fabricate these structural parts or products are supported by elastic restraints or connected to other members, which can also be treated as elastic supports for restraining the plates. Recently, because of its importance, the vibration of elastically restrained laminated composite plates has drawn close attention. For instance, elastically restrained laminated composite plates have been used to fabricate flat-panel sound radiators which can produce full range and high quality sounds [1, 2]. The elastically restrained laminated composite plates of these flat-panel sound radiators vibrate and radiate sounds when excited by an electro-magnetic exciter. The sound quality and radiation efficiency of the flat-panel sound radiators greatly depend on the vibration characteristics of the elastically restrained laminated composite plates. A thorough understanding of the vibration characteristics of the elastically restrained laminated composite plates can help improve the design of such flat-panel sound radiators. On the other hand, the attainment of the actual vibration characteristics of elastically restrained composite plates can enrich the knowledge of the vibration analysis of composite plate structures. Therefore, the determination of accurate vibration characteristics of elastically restrained laminated composite plates is indeed one of the important research topics in the field of composite plate structures.

In the past several decades, free vibration of laminated composite plates with different boundary conditions has been investigated by many researchers and different techniques have been proposed to determine the modal characteristics (natural frequencies and mode shapes) of the plates with regular boundary conditions such as free, simply supported, and fixed edges [3-7]. In reality, plate structures are generally connected to other structural components which can be treated as elastic restraints of the plate structures. Therefore, many researchers have investigated the effects of elastic restraints on the modal characteristics of plates via the theoretical approach [8-12]. For instance, Hao and Kam [11] presented an eigenvalue formulation for the free vibration analysis of symmetrically laminated rectangular plates with different elastic edge and/or interior restraints. In their study, the first 12 natural frequencies and mode shapes of the flexibly restrained plates were determined. Recently, many researchers have studied the sound radiation of plates subjected to vibration [13-18]. For instance, Lomas and Hayek [18] presented a Green function solution to study the steady-state vibration and sound radiation of elastically restrained rectangular plates. They also studied the effects of support conditions on the low frequency sound radiation from a plate. In the previous papers on vibration and sound radiation of plates, it was assumed that the excitation forces were applied directly to the plates and the effects of the exciters used to excite the plates were neglected. As for an electro-magnetic type flat-panel sound radiator, the sound radiation panel of the sound radiator can be treated as an elastically restrained plate. The voice coil assembly of the exciter used to excite the elastically restrained plate for sound radiation is adhesively attached to the bottom surface of the plate. The attachment of the voice coil assembly to the plate should have some effects on the vibration and sound radiation of the plate and such effects may become too significant to be neglected when the size ratio of the length of the panel to the radius of the voice coil gets smaller. Therefore, the vibration characteristics of a flat-panel sound radiator with the inclusion of the voice coil assembly should be properly determined if an accurate prediction of the sound radiation behavior of the radiator is desired. Regarding the optimal design of flat-panel sound radiators, especially those comprising laminated composite sound radiation plates, it seems not much work has been devoted to this area. As the optimal design of a laminated composite flat-panel sound radiator is a time-consuming process, it thus requires a simple yet accurate method for the vibration analysis of the sound radiator if meaningful results are to be obtained in an efficient way. The establishment of a simple and accurate method for vibration analysis of laminated composite flat-panel sound radiators is an important topic of research and more research work should be done in this area.

In this paper, the vibration characteristics of flat-panel sound radiators comprising different elastically restrained laminated composite plates for sound radiation are studied via both theoretical and experimental approaches. Different finite element models are proposed to predict the vibration characteristics of elastically restrained sound radiation plates. The effects of support conditions and size ratio of plate length to voice coil

radius on the vibration characteristics of several elastically restrained laminated composite plates are investigated using the proposed finite element models. Experiments were performed to measure the vibration characteristics of two laminated composite flat-panel sound radiators. The experimental results were used to study the suitability of the finite element models for vibration analysis of laminated composite flat-panel sound radiators.

## 2. Finite Element Formulation of Flat-panel Sound Radiator

Consider the elastically restrained laminated composite sound radiation plate composed of a rectangular laminated composite plate for generating sounds, a flexible edge surround for restraining the vertical motion of the composite plate, an electro-magnetic type exciter for exciting the plate, and a rigid frame for mounting the surround and exciter as shown in Fig. 1. The laminated composite plate of length  $a$ , width  $b$ , and constant thickness  $h$  is composed of  $n$  layer groups of orthotropic laminae with different fiber angles and supported by the elastic edge surround. The plate is excited at the center by the electro-magnetic exciter which consists of a cylindrical voice coil, a magnetic assembly, and a damper. The voice coil of radius  $r_c$  is a cylindrical bobbin of which the top edge is adhesively attached to the bottom surface of the plate and the bottom part of the bobbin is wound by copper wire as shown in Fig. 2. When an electric current passes through the wire, the voice coil will move up and down to excite the plate. The damper is a corrugate and annular membrane which works as a flexible support for restraining the vertical motion of the voice coil. Herein, the voice coil together with the damper is termed as the voice coil assembly. The mathematical model used to analyze the vibration behavior of the elastically restrained laminated composite sound radiation plate is shown in Fig. 3. Herein, the  $x$ - and  $y$ -coordinates of the  $x$ - $y$ - $z$  Cartesian coordinate system are taken in the mid-plane of the plate. The elastic edge surround is modeled as a continuous spring system composed of rotational and translational springs with spring constant intensities  $K_L$  and  $K_R$ , respectively, while the interior damper is a ring-type spring system with radius  $r_c$  composed of translational springs with spring constant intensity  $K_C$ . The center of the interior ring-type spring system is located at the center ( $a/2, b/2$ ) of the plate. The effective mass per unit length,  $m_s$ , of the edge surround is modeled as distributed mass located at the plate edge. The mass intensity  $m_c$  denotes the mass of the voice coil assembly distributed uniformly around the periphery of the contact circle between the plate and the voice coil. Let the maximum deflection, shear rotation in  $x$ -direction, and shear rotation in  $y$ -direction of the plate be  $w(x, y)$ ,  $\theta_x$ , and  $\theta_y$ , respectively. If the coupling between transverse bending and in-plane stretching is neglected, based on the first-order shear deformation theory [19], the maximum strain energies of the laminated composite plate and the voice coil can be expressed in the following form.

$$\begin{aligned}
 U_p = \frac{1}{2} \int_A & \left[ D_{11} \left( \frac{\partial \theta_x}{\partial x} \right)^2 + D_{22} \left( \frac{\partial \theta_y}{\partial y} \right)^2 + 2D_{12} \left( \frac{\partial \theta_x}{\partial x} \right) \left( \frac{\partial \theta_y}{\partial y} \right) \right. \\
 & + 2D_{16} \frac{\partial \theta_x}{\partial x} \left( \frac{\partial \theta_x}{\partial y} \right) \left( \frac{\partial \theta_y}{\partial x} \right) + 2D_{26} \frac{\partial \theta_y}{\partial y} \left( \frac{\partial \theta_x}{\partial y} \right) \left( \frac{\partial \theta_y}{\partial x} \right) + D_{66} \left( \frac{\partial \theta_x}{\partial y} + \frac{\partial \theta_y}{\partial x} \right)^2 \\
 & \left. + A_{44} \left( \frac{\partial w}{\partial y} + \theta_y \right)^2 + 2A_{45} \left( \frac{\partial w}{\partial x} + \theta_x \right) \left( \frac{\partial w}{\partial y} + \theta_y \right) + A_{55} \left( \frac{\partial w}{\partial x} + \theta_x \right)^2 \right] dA
 \end{aligned} \tag{1}$$

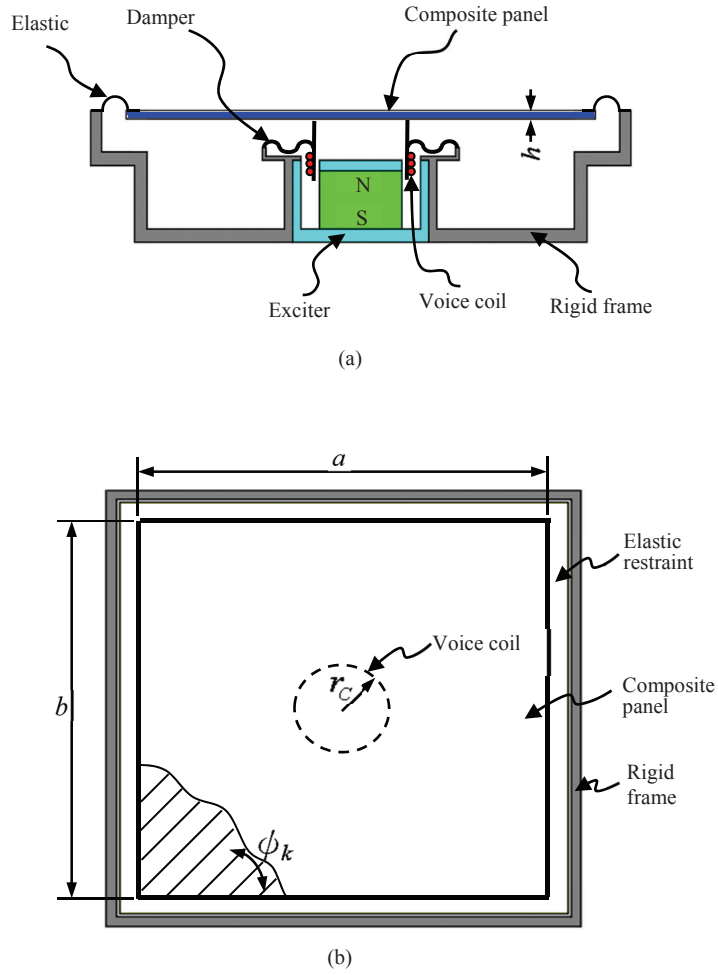


Fig. 1 Elastically restrained laminated composite sound radiation plate: (a) side view. (b) top view.

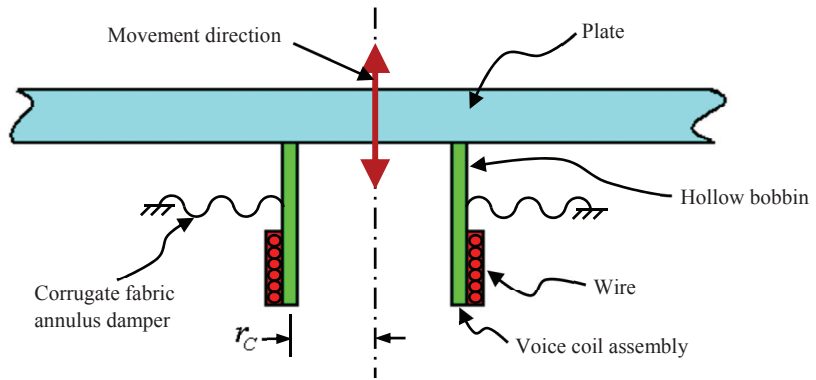


Fig. 2 Voice coil assembly.

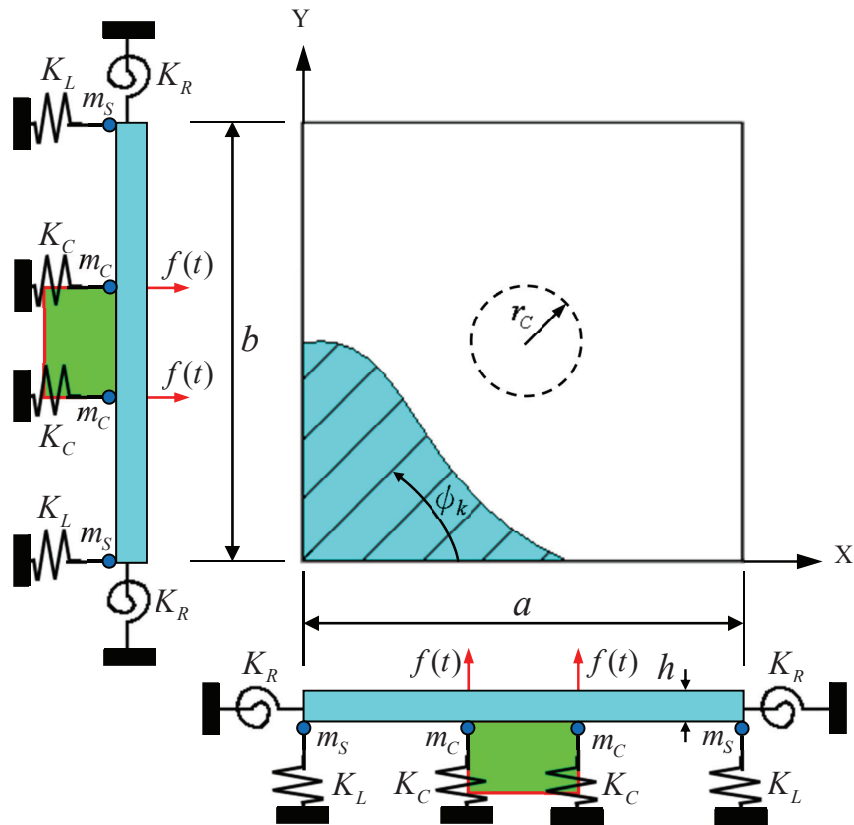


Fig. 3 Mathematical model of elastically restrained laminated composite sound radiation plate.

In the above equation, the bending and shear stiffness coefficients, ie,  $D_{ij}$  and  $A_{ij}$  are given, respectively, as

$$D_{ij} = \frac{1}{3} \sum_{k=1}^n (\bar{Q}_{ij})_k (z_k^3 - z_{k-1}^3) ; \quad i, j = 1, 2, 6 \tag{2}$$

$$A_{ij} = \sum_{k=1}^n (\bar{Q}_{ij})_k (z_k - z_{k-1}) ; \quad i, j = 4, 5$$

where the transformed stiffness coefficients  $(\bar{Q}_{ij})_k$  of the  $k$ th layer group depend on the material properties and fiber orientation of the layer group and are expressed as

$$\begin{aligned}
\bar{Q}_{11} &= Q_{11}c^4 + 2(Q_{12} + 2Q_{66})s^2c^2 + Q_{22}s^4 \\
\bar{Q}_{12} &= (Q_{11} + Q_{22} - 4Q_{66})s^2c^2 + Q_{12}(c^4 + s^4) \\
\bar{Q}_{22} &= Q_{11}s^4 + 2(Q_{12} + 2Q_{66})s^2c^2 + Q_{22}c^4 \\
\bar{Q}_{16} &= (Q_{11} - Q_{12} - 2Q_{66})sc^3 + (Q_{12} - Q_{22} + 2Q_{66})s^3c \\
\bar{Q}_{26} &= (Q_{11} - Q_{12} - 2Q_{66})s^3c + (Q_{12} - Q_{22} + 2Q_{66})sc^3 \\
\bar{Q}_{66} &= (Q_{11} + Q_{22} - 2Q_{12} - 2Q_{66})s^2c^2 + Q_{66}(c^4 + s^4) \\
\bar{Q}_{44} &= Q_{44}c^2 + Q_{55}s^2 \\
\bar{Q}_{55} &= Q_{55}c^2 + Q_{44}s^2 \\
\bar{Q}_{45} &= (Q_{55} - Q_{44})sc
\end{aligned} \tag{3}$$

with

$$\begin{aligned}
Q_{11} &= \frac{E_1}{1 - \nu_{12}\nu_{21}} \quad ; \quad Q_{12} = \frac{\nu_{21}E_2}{1 - \nu_{12}\nu_{21}} \quad ; \quad Q_{22} = \frac{E_2}{1 - \nu_{12}\nu_{21}} \\
Q_{55} &= Q_{66} = G_{12} \quad ; \quad Q_{44} = G_{23}
\end{aligned} \tag{4}$$

where  $E_1$  and  $E_2$  are the Young's moduli in the fiber and transverse directions, respectively;  $\nu_{ij}$  is the Poisson's ratio for transverse strain in the  $j$ th direction when stressed in the  $i$ th direction;  $G_{12}$  is shear modulus in the 1-2 plane;  $G_{23}$  is shear modulus in the 2-3 plane; "s" and "c" represent  $\sin \psi_k$  and  $\cos \psi_k$ , respectively, with  $\psi_k$  being the lamina fiber angle of the  $k$ th layer. It is noted that the displacement compatibility conditions at the interface between the plate and voice coil are observed. The total maximum kinetic energy of the flat-panel sound radiator is

$$T = \frac{\rho_p h \omega^2}{2} \int_0^{a_0} \int_0^{b_0} w^2 dy dx + \frac{\omega^2}{2} \oint_{L_c} m_c w^2 dL + \frac{\omega^2}{2} \oint_{L_s} m_s w^2 dL \tag{5}$$

where  $\omega$  is vibration frequency;  $\rho_p$  is plate mass density per unit area;  $\oint_L$  denotes the integration around the periphery of the plate edge or ring-type support. For the plate with elastic restraints, additional strain energy stored in the translational and rotational springs exists. The maximum strain energy associated with the elastic restraints is

$$U_S = \oint_{L_S} \frac{1}{2} K_T w^2 dL + \oint_{L_S} \frac{1}{2} K_R \theta_n dL + \oint_{L_C} \frac{1}{2} K_C w^2 dL \tag{6}$$

where  $\theta_n$  is the rotation in the direction normal to the plate edge. In view of Eqns (1) and (6), the total strain energy  $U$  of the laminated composite sound radiation plate can be expressed as

$$UT = U_p + U_v + U_S \tag{7}$$

where  $U_p$  and  $U_v$  are strain energies of plate and voice coil, respectively. In the following, the vibration problem of the sound radiation plate is solved using the standard finite element method. The extremization of the functional  $I = UT - T$  with respect to nodal displacements  $\Delta_j$  of the elastically restrained plate leads to the following eigenvalue problem.

$$[\mathbf{K} - \omega^2 \mathbf{M}] \Delta = \mathbf{0} \quad (8)$$

where  $\mathbf{K}$  and  $\mathbf{M}$  are stiffness and mass matrices of the sound radiation plate, respectively;  $\Delta$  is the column vector collecting the structural nodal displacements. The modal characteristics (natural frequencies and mode shapes) of the plate can then be determined from Eqn (8).

In the force vibration analysis, the equations of motion for the sound radiation plate can be expressed in matrix form as

$$\mathbf{M}\ddot{\Delta} + \mathbf{C}\dot{\Delta} + \mathbf{K}\Delta = \mathbf{F} \quad (9)$$

where  $\mathbf{C}$  is the structural damping matrix,  $\dot{\Delta}$  the nodal velocity vector,  $\Delta$  the nodal acceleration, and  $\mathbf{F}$  the force vector. The damping matrix is related to  $\mathbf{M}$  and  $\mathbf{K}$  as [20]

$$\mathbf{C} = \alpha \mathbf{M} + \beta \mathbf{K} \quad (10)$$

where  $\alpha$  and  $\beta$  are constants determined experimentally.

The excitation force  $F_v$  exerted to the plate through the voice coil can be determined using the following equation.

$$F_v = B \times L \times I \quad (11)$$

where  $B$  is magnetic flux density,  $L$  is the length of the copper wire of the voice coil submerged in the magnetic field, and  $I$  is electric current.

Herein, the finite element code ANSYS [21] is used to solve Eqns (8) and (9). The schematic description of the finite element model of the sound radiation plate is shown in Fig. 4 in which SHELL 91 elements are used to model the laminated composite plate and voice coil, MASS 21 to model distributed masses, and COMBIN 14 elements to model the springs. In the free vibration analysis, the MODAL module is used to determine the natural frequencies and mode shapes of the sound radiation plate. In the force vibration analysis, the HARMONIC module is used to determine the amplitudes and phase angles at the nodes of the plate excited by a harmonic load with a given excitation frequency. Once the amplitudes of the nodes are known, the nodal lines, where the amplitudes are zero, of the vibration shape of the plate can be constructed.

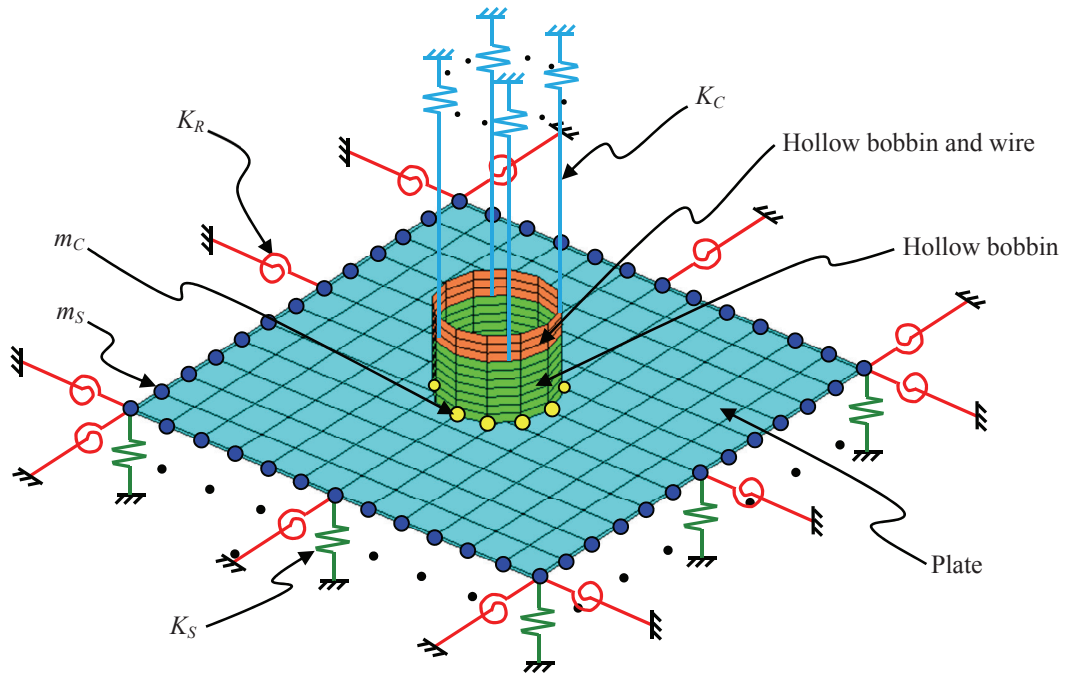


Fig. 4 Finite element model of elastically restrained laminated composite sound radiation plate.

### 3. Experimental Investigation

The vibration characteristics of sound radiation plates composed of square Gr/ep  $[0^\circ/90^\circ]_s$  laminated composite plates with free edge and a voice coil assembly of radius  $r_c = 12.75$  mm at the plate center were studied experimentally. The length and thickness of the square laminated composite plates were 103.4 mm and 0.58 mm, respectively, and the size ratio  $a / r_c = 8.1$ . Regarding the voice coil, the height and thickness of the bobbin were 20 mm and 0.15 mm, respectively; the copper wire diameter was 0.17 mm and the winding height was 6 mm. The average material properties of the plate and voice coil (bobbin and copper wire) determined experimentally are given as

Composite plate:

$$\begin{aligned} E_1 &= 115.05 \text{ GPa}, & E_2 &= 7.84 \text{ GPa} \\ G_{12} = G_{13} &= 4.10 \text{ GPa}, & G_{23} &= 0.674 \text{ GPa} \\ \nu_{12} &= 0.306, & \rho_p &= 1403 \text{ kg/m}^3 \end{aligned}$$

Bobbin:

$$E_v = 19.35 \text{ GPa}, \quad \nu_v = 0.33 \quad (12)$$

Copper wire:



$$E_c = 101.0 \text{ GPa}, \quad \nu_c = 0.35$$

The spring constant and mass of the interior ring-type support were determined experimentally by measuring the resonant frequency, mass, and spring constant of the exciter using the sound measurement software MLSSA [22]. For the ring-type spring system of radius  $r_c = 12.75$  mm, the experimentally determined spring constant intensities were  $K_c = 1.4394 \times 10^4$  N/m<sup>2</sup> and  $1.3778 \times 10^4$  N/m<sup>2</sup> for the  $[0^\circ/90^\circ]_s$  sound radiation plates, respectively. The mass per unit length at the plate center was  $m_c = 17.30$  kg/m.

The plates were subjected to sweep sine excitation using the exciter in Fig. 1 and the measured vibration data were used to construct the frequency response spectra of the plates. The experimental setup for vibration study of the sound radiator is shown in Fig. 5. In the vibration testing of the sound radiator, the B&K 3650C data acquisition system was used to provide a series of harmonic sine function signals sweeping in a specific frequency range to the electro-magnetic exciter to make the plate vibrate. The plate response signals picked up by the laser gun (OFV 350) and vibrometer (OFV 2500) were analyzed using the FFT analyzer of the B&K 3650C data acquisition system to construct the frequency response spectrum of the plate. The damped natural frequencies of the flexibly supported plate were then extracted from the measured frequency response spectrum by identifying the peaks of the spectrum. The  $i^{\text{th}}$  modal damping ratio  $\zeta_i$  was approximated using the relation  $\zeta_i = 1/2Q_i$  where  $Q_i$  is the quality factor of the  $i$ th mode. The  $i^{\text{th}}$  undamped natural frequency  $f_i$  was determined using the relation  $f_i = f_{id} (1 - \zeta_i^2)^{-1/2}$  where  $f_{id}$  is the  $i$ th damped natural frequency. It is noted that the natural frequencies of the plate with nodal lines passing through the plate center cannot be identified from the frequency response spectrum. The constants  $\alpha$  and  $\beta$  in Eqn (10) determined using the 1<sup>st</sup> and the 15<sup>th</sup> experimental modal damping ratios were 0.10317 and 0.09922, respectively. The laser gun was also placed at different locations to measure the plate responses for identifying the vibration shapes associated with the natural frequencies. One easy way to identify the vibration shape was to locate the nodal lines on the plate. The other way used in this study to identify the nodal lines was the salt powder spraying technique. In this test, small amount of salt powder of weight less than 0.5g was uniformly scattered on the plate surface. When the plate was excited at a particular frequency, the salt powder would move and gather together along the nodal lines where the displacements were zero.

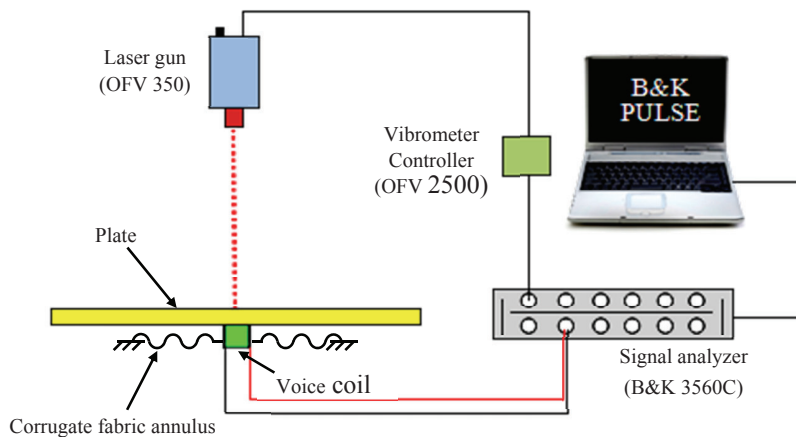


Fig. 5 Vibration test apparatus.

#### 4. Results and Discussions

The present finite element formulation is used to predict the natural frequencies and vibration shapes of the laminated composite sound radiation plate which has been tested. A convergence study has first been performed to determine the appropriate numbers of MASS 21, COMBIN 14, and SHELL 91 elements for modeling the elastically restrained sound radiation plate so that the solution of the eigenvalue problem of Eqn (7) can converge. In this study, for comparison purpose and searching for the simplest model for vibration analysis, the following simplified finite element models are also used to predict the vibration characteristics of the sound radiation plates.

Model I: The bending stiffness of the voice coil is neglected.

Model II: The bending stiffness as well as the mass of the voice coil is neglected.

Model III: The voice coil assembly (bending stiffness, mass, and elastic restraint) is removed.

The results obtained using the above finite element models will be used to study the effects of voice coil assembly parameters on the vibration characteristics of the sound radiation plates.

For the  $[0^\circ/90^\circ]_s$  sound radiation plate with size ratio  $a/r_c = 8.1$  or 4, the first 10 natural frequencies predicted using the finite element models and the available experimental natural frequencies are listed in Table 1 for comparisons. As mentioned before, the modes with nodal lines passing through the center of the plate cannot be induced by the exciter location. Therefore, the experimental natural frequencies associated with these modes are not shown in the table. Regarding the plate of  $a/r_c = 8.1$ , the results given in Table 1 show that the theoretical natural frequencies predicted using the present “full” finite element model are in good agreement with the experimental results and the maximum percentage difference between the theoretical and experimental results is less than 4.8%. However, if the simplified models are used, much higher percentage differences are obtained. For instance, the absolute maximum percentage differences produced by Models I, II, and III are 10.44, 11.1, and 10.98%, respectively. It is noted that all the simplified models are unable to predict the ninth natural frequency for the sound radiation plate. Furthermore, Model I is also unable to predict the first natural frequency because there is no restraint to support the plate. Such results have demonstrated the significant effects of voice coil assembly on the natural frequencies of the laminated composite sound radiation plate and inappropriate modeling of the voice coil assembly may lead to erroneous results. Regarding the  $[0^\circ/90^\circ]_s$  plate of  $a/r_c = 4$ , if the natural frequencies predicted using the present full finite element model are treated as the true values, the absolute maximum percentage errors predicted by Models I, II, and III are 27.8, 32.17, and 32.16%, respectively. Furthermore, the maximum number of natural frequencies for which the simplified models unable to predict increases from two to four. This further reinforces the claim that the voice coil assembly has significant effects on the natural frequencies of the laminated composite sound radiation plate and the effects become larger as the size ratio gets smaller. In determining the theoretical vibration shape, the plate is excited using a harmonic load at the chosen frequency and the HARMONIC Module of ANSYS is used to determine the nodal amplitudes and phases which are then used to construct the vibration shape of the plate. First consider the plate of  $a/r_c = 8.1$ , the nodal lines of the measured vibration shapes are tabulated in Table 2 in comparison with the vibration shapes determined using the present finite element formulation with different degrees of simplification. It is noted that the nodal lines of the theoretical vibration shapes determined using the proposed full finite element model are in good agreement with those of the measured vibration shapes. In contrast, except the first 4 vibration shapes, all the simplified models are unable to predict vibration shapes close to the measured vibration shapes. Regarding the  $[0^\circ/90^\circ]_s$  plate of  $a/r_c = 4$ , if the vibration shapes predicted using the present full finite element model are treated as the true shapes, it is noted that the vibration shapes predicted by the simplified models are completely different from those of the true ones. Such results have further demonstrated the significant effects of the voice coil assembly on the vibration shapes of the laminated composite sound radiation plate and inappropriate modeling of the voice coil assembly may lead to erroneous results. Therefore, the whole voice coil assembly should be included in the vibration and sound radiation analyses of flat-panel sound radiators.




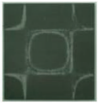



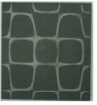
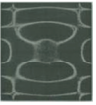
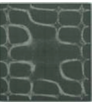
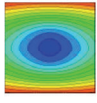
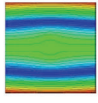
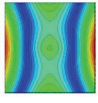
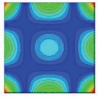
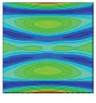
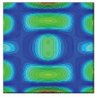
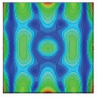
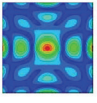
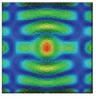
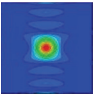
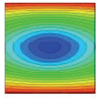
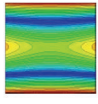
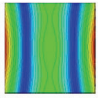
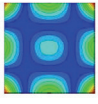
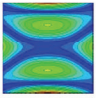
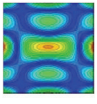
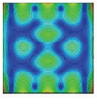
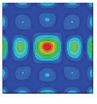
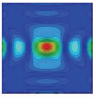
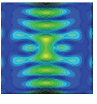
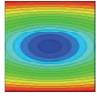
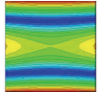
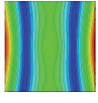
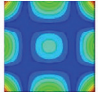
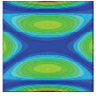
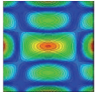
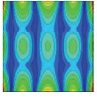
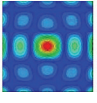
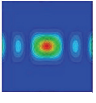
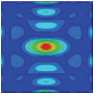
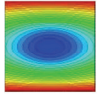
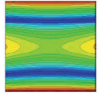
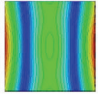
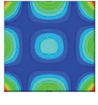
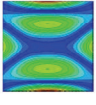
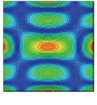
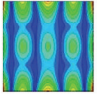
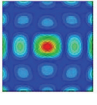
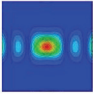
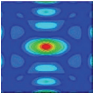
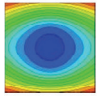
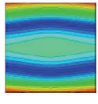
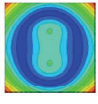
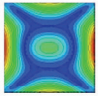
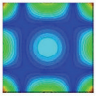
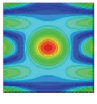
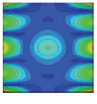
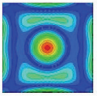
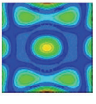
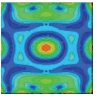
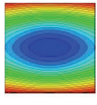
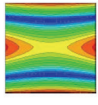
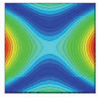
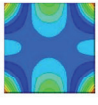
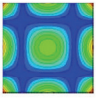
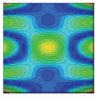
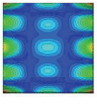
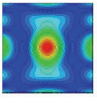
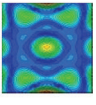
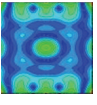
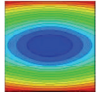
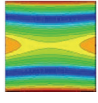
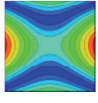
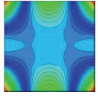
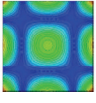
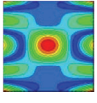
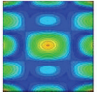
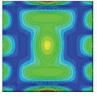
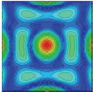
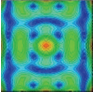
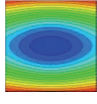
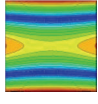
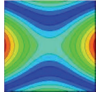
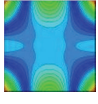
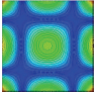
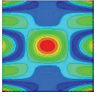
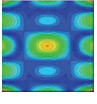
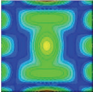
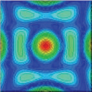
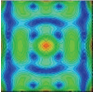
Table 1. Natural frequency of centrally supported  $[0^\circ/90^\circ]$ s sound radiation plate ( $a/b=1$ ,  $a/rc=8.1$ , 4)

a/rc	Mode number	Natural frequency (Hz)									
		1	2	3	4	5	6	7	8	9	10
8.1	Experimental (true)	46.88	207.5	411.3	565.6	946.3	1455	2350	3025	3425	4372
	Present FEM	46.936	207.24	412.73	566.45	954.18	1422.3	2286.3	2897.6	3336.9	4163.5
	Percentage difference	(-0.12)*	(0.13)	(-0.35)	(-0.15)	(-0.83)	(2.25)	(2.71)	(4.21)	(2.57)	(4.77)
	Simplified Model I	46.664	189.06	401.49	561.30	1011.2	1303.1	2135.6	2877.8	—	4258.3
	Percentage difference	(0.46)	(8.89)	(2.39)	(0.76)	(-6.86)	(10.44)	(9.12)	(4.87)	—	(2.60)
	Simplified Model II	49.001	202.18	429.27	596.62	1051.3	1343.7	2286.2	2897.5	—	4051.7
	Percentage difference	(-4.52)	(2.564)	(-4.37)	(-5.48)	(-11.10)	(7.65)	(2.71)	(4.21)	—	(7.33)
	Simplified Model III	— <sup>#</sup>	194.40	425.42	593.12	1050.2	1342.8	2285.7	2897.4	—	4051.6
Percentage difference	—	(6.31)	(-3.43)	(-4.87)	(-10.98)	(7.71)	(2.74)	(4.22)	—	(7.33)	
4	Present FEM (true)	82.125	784.04	1122.8	1985.1	2254.6	4298.6	4658.2	6370.7	8271.4	8919.0
	Simplified Model I	82.284	659.91	—	1433.3	2168.2	4607.8	—	7143.8	8379.7	9202.1
	Percentage difference	(-0.19)	(15.83)	—	(27.80)	(3.83)	(-7.19)	—	(-12.14)	(-1.31)	(-3.17)
	Simplified Model II	99.682	732.97	—	1593.6	2213.8	5001.7	—	8420.3	8832.2	—
	Percentage difference	(-21.38)	(6.51)	—	(19.72)	(1.81)	(-16.36)	—	(-32.17)	(-6.79)	—
	Simplified Model III	—	728.56	—	1591.5	2213.4	5001.0	—	8419.8	8832.8	—
	Percentage difference	—	(7.08)	—	(19.83)	(1.83)	(-16.34)	—	(-32.16)	(-6.79)	—

\* The value in the parentheses denotes the percentage difference between the true and theoretical natural frequencies, ie,  $[(\text{true value} - \text{theoretical value})/\text{experimental value}] \times 100\%$ .

<sup>#</sup>Not available

Table 2. Vibration shape of centrally supported  $[0^\circ/90^\circ]$ s sound radiation plate ( $a/b = 1$ ,  $a/rc = 8.1, 4$ )

$a/rc$	Mode number	1	2	3	4	5	6	7	8	9	10
	Excitation frequency	46.88	207.5	411.3	565.6	946.3	1455	2350	3025	3425	4372
	Experimental (true)										
	Present FEM										
8.1	Simplified Model I										
	Simplified Model II										
	Simplified Model III										
	Excitation frequency	82.125	784.04	1122.8	1985.1	2254.6	4298.6	4658.2	6370.7	8271.4	8919.0
	Present FEM (true)										
4	Simplified Model I										
	Simplified Model II										
	Simplified Model III										

## 5. Conclusions

The vibration characteristics of elastically restrained laminated composite sound radiation plates have been studied via both theoretical and experimental approaches. A centrally restrained laminated composite sound radiation plate of layups  $[0^0/90^0]_s$  was tested to measure the natural frequencies and vibration shapes of the plate. Different finite element models have been presented for analyzing the vibration characteristics of the laminated composite flat-panel sound radiation plate which has been tested. The suitability of the proposed full finite element model with the inclusion of all the parameters of the voice coil assembly in predicting the natural frequencies and vibration shapes of the sound radiators has been validated by the experimental results. The maximum percentage difference between the theoretical natural frequencies predicted using the proposed full finite element model and the experimental ones is 4.77% for the  $[0^0/90^0]_s$  sound radiation plate. A number of simplified finite element models have also been used to predict the vibration characteristics of the sound radiation plates. It has been shown that the neglect of portion or whole parameters of the voice coil assembly in the finite element formulation can produce erroneous predictions of the natural frequencies as well as the vibration shapes for the sound radiators. For these cases, the maximum percentage difference between the theoretical and experimental natural frequencies can be as high as 11.1%. The results obtained in this paper can serve as benchmarks for verifying the correctness of any model for vibration analysis of elastically restrained laminated composite sound radiation plates.

## Acknowledgements

This work was supported by the National Science Council of the Republic of China under Grant NSC 101-3113-S-009-002.

## References

- [1] Kam, T. Y., 2010. Moving-coil planar speaker, U. S. A. Patent Pub. No. US2009/ 0290748 A1.
- [2] Kam, T. Y., 2006. Rectangular Panel-Form Loudspeaker and Its Radiating Panel, U. S. A. Patent No. US7010143.
- [3] Ashton, J. E., 1969. "Natural modes of free-free anisotropic plates", *The Shock and Vibration Bulletin* 39, pp. 93-100.
- [4] Leissa, A. W., 1973. "The free vibration of rectangular plates", *Journal of Sound and Vibration* 31, pp. 257-293.
- [5] Pandit, M. K., Haldar, S., Mukhopadhyay, M., 2007. "Free vibration analysis of laminated composite rectangular plate using finite element method", *Journal of Reinforced Plastics and Composites* 26 (1), pp. 69-80.
- [6] Secgin, A., Sarigul, A. S., 2008. "Free vibration analysis of symmetrically laminated thin composite plates by using discrete singular convolution (DSC) approach: Algorithm and verification", *Journal of Sound and Vibration* 315 (1-2), pp. 197-211.
- [7] Lee, J. M., Chung, J. H., Chung, T. Y., 1997. "Free vibration analysis of symmetrically laminated composite rectangular plates", *Journal of Sound and Vibration* 199 (1), pp. 71-85.
- [8] Hung, K. C., Lim, M. K., Liew, K. N., 1993. "Boundary beam characteristics orthonormal polynomials in energy approach for vibration of symmetric laminates-II: Elastically restrained boundaries", *Composite Structures* 26, pp. 185-209.
- [9] Al-Obeid, A., Copper, J. E., 1995. "A Rayleigh-ritz approach for the estimation of the dynamic properties of symmetric composite plates with general boundary conditions", *Composites Science and Technology* 53, pp. 289-299.
- [10] Nallim, L. G., Luccioni, B. Grossi, M., R. O., 2005. "Vibration of general triangular composite plates with elastically restrained edges", *Twin-Walled Structures* 43 (11), pp. 1711-1745.
- [11] Hou, W. F., Kam, T. Y., 2009. "Modal characteristics of composite plates elastically restrained at different locations", *Int'l Journal of Mechanical Science* 51, pp. 443-452.
- [12] Setoodeh, A. R., Karami, G., 2003. "A solution for the vibration and buckling of composite laminates with elastically restrained edges", *Composite Structures* 60 (3), pp. 245-253.
- [13] Jeyaraj, P., 2010. "Vibro-acoustic behavior of an isotropic plate with arbitrarily varying thickness", *European Journal of Mechanics A-Solids* 29 (6), pp. 1088-1094.
- [14] Putra, A., Thompson D. J., 2010. "Sound radiation from rectangular baffled and unbaffled plates", *Applied Acoustics* 71 (12), pp. 1113-1125.
- [15] Zhang, X. F., Li, W. L., 2010. "A unified approach for predicting sound radiation from baffled rectangular plates with arbitrary boundary conditions", *Journal of Sound and Vibration* 329 (25), pp. 5307-5320.
- [16] Yoo, J. W., 2010. "Study on the general characteristics of the sound radiation of a rectangular plate with different boundary edge conditions", *Journal of Mechanical Science and Technology* 24 (5), pp. 1111-1118.

- [17] Hashemi, S. H., Khorshidi, K., Taher, H. R. D., 2009. "Exact acoustical analysis of vibrating rectangular plates with two opposite edges simply supported via Mindlin plate theory", *Journal of Sound and Vibration* 322 (4-5), pp. 883-900.
- [18] Lomas, N. S., Hayek, S. I., 1977. "Vibration and acoustic radiation of elastically supported rectangular plates", *Journal of Sound and Vibration* 52 (1). pp. 1-25.
- [19] Reddy, J. N., 1984. "A Simple Higher Order Theory for Laminated Composite Plates", *Journal of Applied Mechanics* 51 (4), pp. 745–752.
- [20] Harris, C. M., Crede, C. E., 1976. *Shock and vibration handbook*, McGraw-Hill, Inc.
- [21] ANSYS 12.1, ANSYS, Inc., USA, 2010.
- [22] MLSSA-Acoustical Measurement System, DRA Laboratories, Sarasota, FL, USA, 1987.